Measurement of 0.35-μm Laser Imprint in a Thin Si Foil Using an X-Ray Laser Backlighter

D. H. Kalantar
*M. H. Key**
L. B. DaSilva
S. G. Glendinning
*J. P. Knauer***
B. A. Remington
F. Weber
S. V. Weber

Introduction

High-gain direct-drive inertial confinement fusion (ICF) requires very uniform irradiation of a hollow spherical shell with a layer of fusionable deuterium–tritium (D-T) on its inner surface. The intensity of laser irradiation builds up in several nanoseconds from an initial "foot" at 10^{13} W/cm^2 to more than 10^{15} W/cm^2 during the main drive pulse. Laser ablation of the capsule surface produces a high pressure that accelerates the shell radially inward in a spherical implosion. During the main drive phase, there is Rayleigh–Taylor (RT) growth of surface perturbations due to two factors: the initial surface roughness of the capsule and imprint from spatial nonuniformities in the laser drive intensity early in the laser pulse. With the completion of the Omega upgrade laser at the University of Rochester,[1] the Nike laser at the Naval Research Laboratory,[2] and proposals for the National Ignition Facility (NIF),[3] there is considerable interest in studying the physics of direct-drive ICF, and particularly in the imprinting process.[4–6]

On a large scale, the uniformity of illumination on a direct-drive implosion capsule is determined by the multibeam irradiation geometry, and on a small scale, by beam smoothing techniques. Large-scale nonuniformities are minimized by using a large number of beams (such as the 60 beams of the Omega Upgrade laser or 48 beam clusters of the proposed NIF). The small-scale spatial variations of intensity due to the speckle pattern of individual laser beams are effectively smoothed with smoothing by spectral dispersion (SSD),[7] where a random phase plate (RPP)[8] is illuminated by the spectrally dispersed frequency components of a broad-band laser beam giving a rapidly fluctuating speckle pattern on the target.

Our interest is in studying the imprinting of nonuniformities due to a direct-drive laser beam under conditions simulating the low-intensity foot of a pulse designed for an ignition target such as might be used on the NIF. By studying the reduction of optical and imprinted hydrodynamic perturbations with SSD smoothing, we will be able to assess the effectiveness of SSD bandwidth in suppressing imprint for direct-drive experiments. To demonstrate the effect of beam smoothing on laser imprint, we have obtained extreme ultraviolet (XUV) radiographs (at 15.5-nm radiation) of the imprinted modulation at shock breakout due to (1) a static laser speckle pattern and (2) a one-dimensional (1-D) SSD smoothed speckle pattern.

Experiment

We irradiated a 3-μm-thick Si foil with a 3×10^{12}-W/cm^2, 400-ps pulse of 0.35-μm laser light in the Nova two-beam target chamber.[9] The speckle pattern from this beam imprinted modulations in the Si foil, which we measured by XUV radiography. We used an Y x-ray laser with a wavelength of 15.5 nm as the XUV backlighter,[10,11] and we imaged the Si foil in two dimensions onto an XUV-sensitive charge-coupled device (CCD) camera by using XUV multilayer optics[12] as shown in Fig. 1.[13–15] The XUV imaging system uses an off-axis spherical optic for imaging at about 25× magnification. The angle of incidence on the imaging optic was only 1.25°, minimizing astigmatism, and providing a spatial resolution of about 3 μm.

The XUV image is a two-dimensional (2-D) image of the modulation in optical depth of the foil at 15.5 nm due to imprint of the laser speckle pattern. We used the x-ray laser as a backlighter since the optical depth of most materials is high at 15.5 nm, which allows us to make a sensitive measurement of the optical depth variation in the foil. Si was used because it has the lowest

*Rutherford Appleton Laboratory, UK, and University of Oxford, UK.
**University of Rochester, Laboratory for Laser Energetics, Rochester, New York.

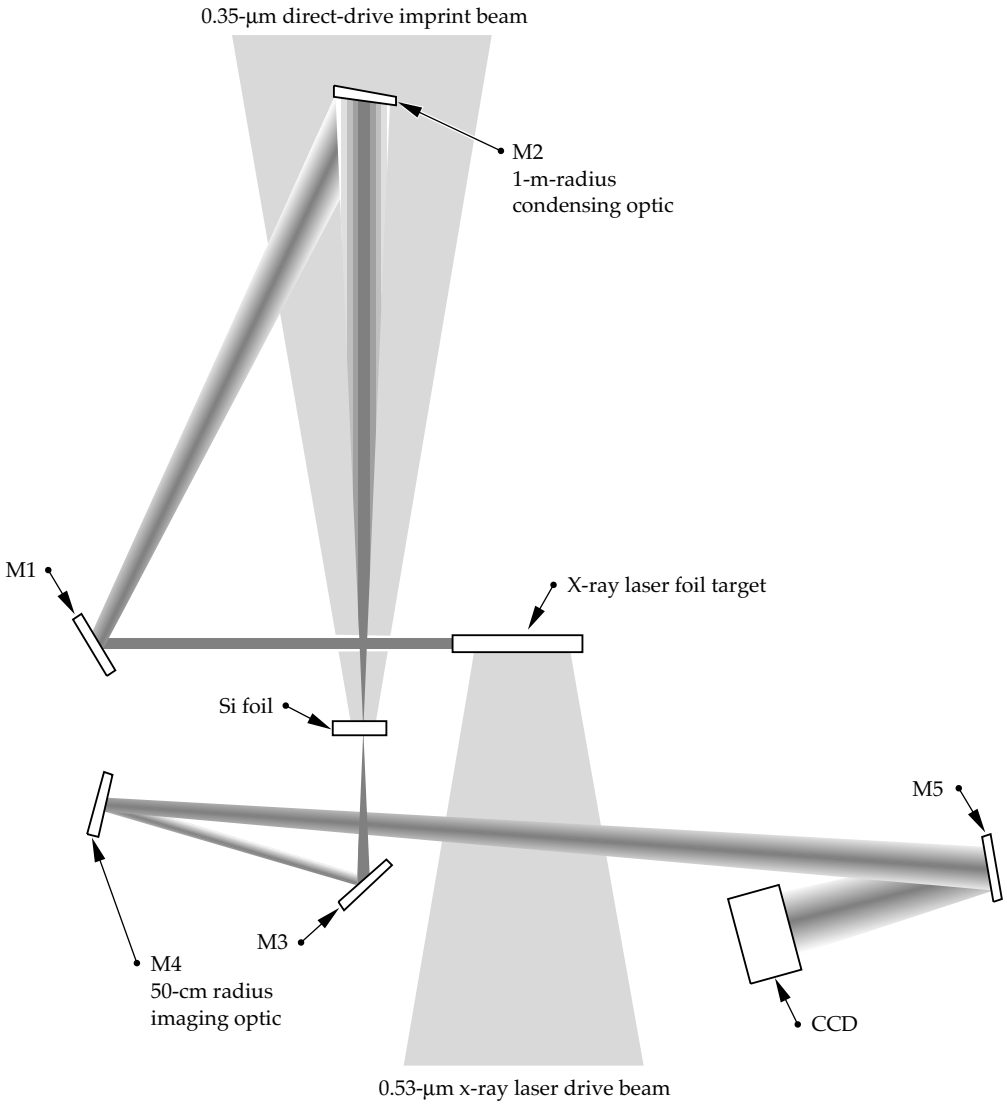

FIGURE 1. X-ray laser imaging system for measuring direct-drive imprinted modulation on a thin Si foil. The imaging optics are Mo/Si multilayer optics. (08-00-0296-0363pb01)

opacity at 15.5 nm. It is still highly attenuating at this wavelength, which limits the thickness of foils that we can probe to <4 μm. Because it is highly attenuating, a 50-nm thickness variation in the Si foil results in a 10% change in the backlighter intensity in the XUV radiograph.

To measure the effect of laser imprint on a directly driven foil, we probe the foil before significant RT growth occurs at the time of shock breakout. Computer simulations of the Si foil done with the LASNEX computer code[16] indicate that with a laser intensity of 3×10^{12}-W/cm^2, a ~2-Mbar shock propagates through a 3-μm-thick foil and breaks out the back side at about 260 ps. At this time, the Si foil is compressed by a factor of 1.5. We timed the 80 ps duration x-ray laser pulse to radiograph the optical depth modulation of the foil at shock breakout, namely at t = 260 ps, and we turned the optical laser drive pulse off at 400 ps.

Laser Imprint

In Fig. 2, we show time-integrated far-field images of the drive beam that were recorded photographically at an equivalent focal plane diagnostic station. These are shown as modulation in the intensity pattern of the RPP focal spot. Figure 2(a) shows the static RPP speckle pattern for a 100-μm-square region at the object plane obtained with zero bandwidth. The theoretical root mean square (rms) fractional modulation of the exposure due to a static RPP speckle pattern is 1.0.[17] We measured a modulation of 0.6, but our measurement may be affected by the finite resolution of the far field imaging system, the film calibration, and the fact that the beam has a time-skew of about 100 ps. Note that the time skew is introduced by the grating used to disperse the bandwidth for SSD. It results in a

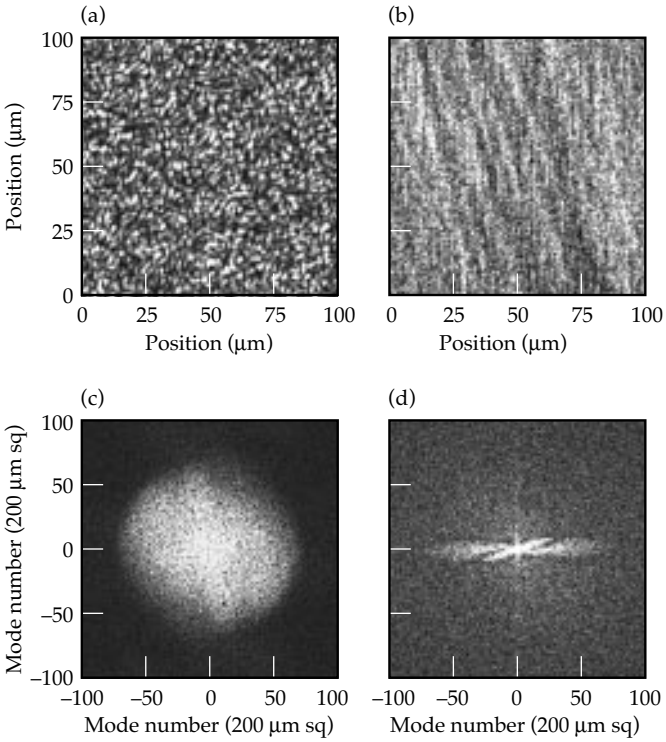

FIGURE 2. Time-integrated optical far-field images of the 0.35-μm laser intensity modulation in a 100-μm-square region at the equivalent focal plane for (a) a static speckle pattern with an intensity of 2.3×10^{12} W/cm^2 and (b) an SSD-smoothed speckle pattern with 0.33 THz of bandwidth at 0.35 μm and an intensity of 3.3×10^{12} W/cm^2. Two-dimensional Fourier transforms of (c) the static speckle pattern and (d) the SSD-smoothed speckle pattern shown for a 200-μm-square region of the object plane. (08-00-0296-0364pb01)

speckle pattern that changes during the initial portion of the laser pulse as the laser beam fills in to the full aperture, even for the case with no bandwidth.

The optical far-field image shown in Fig. 2(b) for the case of 0.33-THz bandwidth at 0.35 μm has an rms modulation of 0.15. This is the time-integrated modulation in exposure. This value is reduced from a theoretical value of 1.0 for the static speckle pattern by the SSD. It reaches an asymptotic value of 0.15 after about 100 ps. One-dimensional streaks in the vertical direction are due to the 1-D dispersion from the grating, and additional streaks at a small angle relative to the vertical are attributed to chromatic aberration in the focus lens, resulting in a multidirectional SSD pattern.

We characterize the far-field speckle pattern by Fourier analysis. Figures 2(c) and 2(d) show 2-D Fourier transforms of the far-field intensity modulation. The transform of the static laser speckle pattern shows azimuthal symmetry due to the isotropy of the speckle pattern [Fig. 2(c)]. The transform of the SSD-smoothed speckle pattern, however, has a distinct "propeller" shape that dominates in the horizontal direction [Fig. 2(d)]. This indicates that there is short-wavelength structure in the horizontal direction [i.e., perpendicular to the vertical streaks in Fig. 2(b)], while short-scale laser nonuniformities are suppressed in the vertical direction due to the SSD smoothing. The transform also shows a feature that is tilted at about 20°. This is due to the slightly rotated additional streaks in Fig. 2(b), mentioned above.

Figure 3 shows face-on radiography images of the imprinted modulation in thin Si foils due to both a static speckle pattern and an SSD-smoothed speckle. The imprint appears as a modulation in the optical depth of the foil, given by the natural logarithm of the ratio of transmitted XUV intensity to a smoothed fit of the overall x-ray laser profile. Figure 3(a) shows a 100-μm-square region from the radiograph of a 3.05-μm-thick Si foil irradiated by the static speckle pattern shown in Fig. 2(a). Figure 3(b) shows a 100-μm-square region from the radiograph of a 3.15-μm-thick Si foil irradiated by the SSD-smoothed speckle pattern shown in Fig. 2(b).

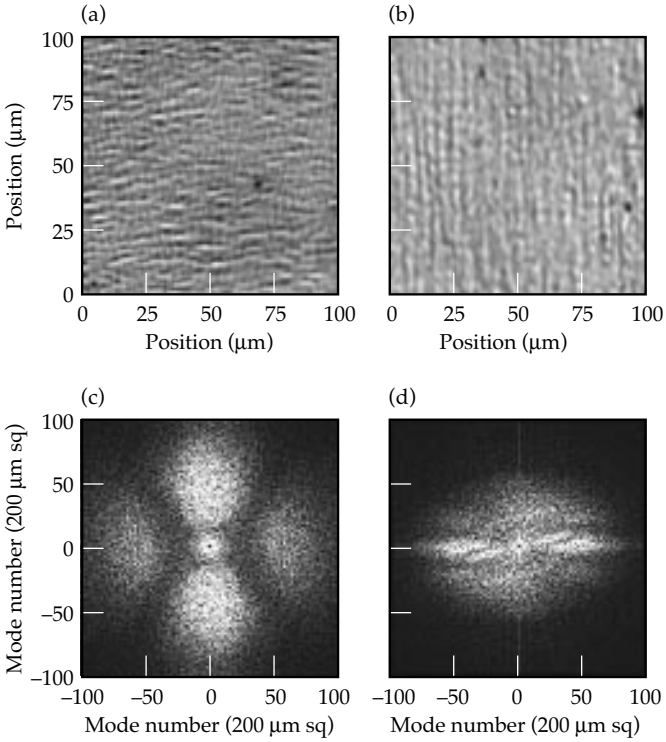

FIGURE 3. XUV radiographs showing the imprinted modulation in optical depth in a 100-μm-square region at the object plane of (a) a 3.05-μm Si foil irradiated by the speckle pattern shown in Fig. 2(a) and (b) a 3.15-μm Si foil irradiated by the SSD-smoothed speckle pattern shown in Fig. 2(b). These radiographs were obtained at t = 260 ps. Two-dimensional Fourier transforms of the imprint due to (c) a static speckle pattern and (d) an SSD-smoothed speckle pattern shown for a 200-μm-square region of the object plane. (08-00-0296-0365pb01)

The rms modulation in optical depth of the foil imprinted with a static speckle pattern is 0.37 ± 0.06. We translate this to an rms modulation in foil thickness using the cold opacity, μ, times the density of Si, ρ. The shocked density of the Si foil is about 1.5 times solid density at shock breakout, which gives us a product $\mu\rho = 3.21\ \mu m^{-1}$. Therefore, this modulation in optical depth corresponds to an rms thickness modulation of only 115 nm in the foil at shock breakout.

The rms modulation in optical depth of the Si foil imprinted with the 0.33-THz SSD-smoothed beam is 0.23 ± 0.04, which corresponds to a 72-nm rms modulation. The error bars quoted above correspond to the standard deviation obtained from calculating the rms from multiple lineouts of the 2-D radiographs.

Figures 3(c) and 3(d) show 2-D Fourier transforms of the face-on XUV radiographs. The Fourier transform corresponding to the static speckle pattern [Fig. 3(c)] shows a lobe structure with the vertical direction dominating. This is a result of the slight horizontal anisotropy in the radiograph image [Fig. 3(a)], and is consistent with the astigmatism of the imaging system when the foil is about 100 μm away from best focus,[15] which is the limit of our ability to position the Si foil. Note that the uncertainty in the measured rms optical depth modulation due to locating the target to within 100 μm of best focus of the imaging system is ±20%.

Figure 3(d) shows the Fourier transform of the optical depth modulation imprinted with the SSD-smoothed speckle pattern. One-dimensional SSD suppressed the short-wavelength structures in the direction of dispersion. As a result, the 2-D Fourier transform shows structures similar to the Fourier transform of the intensity modulation of the laser speckle intensity pattern [Fig. 2(d)]. The transform has a strong directionality, and the tilted structure due to chromatic aberrations of the Nova lens is reproduced in imprint almost identically.

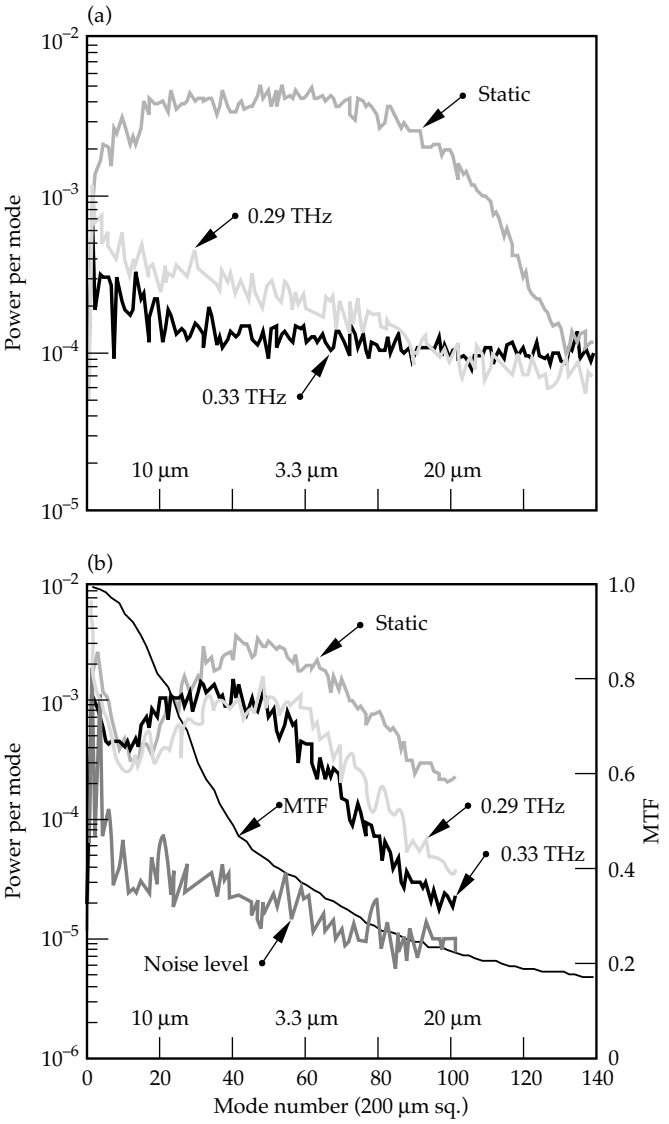

FIGURE 4. Power per mode for a 200-μm region measured from (a) the optical far-field images and (b) the XUV radiographs of 0.35-μm laser imprint. The MTF for the imaging system is shown overlaid in (b). (08-00-0296-0366pb01)

Discussion and Simulations

We compare the modulations imprinted in the Si foil with and without SSD bandwidth by performing radial lineouts of the square of the 2-D Fourier transforms (Fourier power) of the optical speckle patterns and the XUV radiographs of the imprinted foils, as shown in Fig. 4. We azimuthally integrated the Fourier power so that the sum over mode number gives us the square of the rms. Figure 4(a) shows the Fourier power per mode calculated for the static and 0.33-THz SSD band width cases. We also show the result for an intermediate case of 0.29-THz (at 0.35 μm) SSD bandwidth, obtained on a separate shot. Figure 4(b) shows the Fourier power per mode for the XUV radiographs recorded at the time of shock breakout with zero, 0.29-THz, and 0.33-THz SSD bandwidth. The noise in the radiograph measurement is shown as a power spectrum calculated from the XUV radiograph of an undriven Si target. The noise is primarily due to the surface finish of the polished Si foils, which we characterized by scanning with an atomic force microscope. Note that we have also plotted a modulation transfer function (MTF) for the imaging system in Fig. 4(b) to illustrate the resolution at short wavelengths. The calculated value of the MTF is about 0.3 for a 3-μm wavelength modulation.

The modulation of optical depth at 15.5 nm in the Si foil has an rms of about 0.37 ± 0.06 when it is imprinted with a static 0.35-μm laser speckle pattern. The rms is reduced by 40% to 0.23 ± 0.04 when we apply 0.33-THz SSD beam smoothing on the imprint beam. The reduction in power per mode is greatest for the short wavelength modes ($n \geq 40$, $\lambda < 5\ \mu m$). For a mode number of 67 ($\lambda = 3\ \mu m$), the power is reduced by a factor of six. For

a mode number of 20 (λ = 10 μm), the power is nearly the same with and without bandwidth, differing by at most 50%. The time-integrated modulation in fractional exposure of the speckle pattern shows a much greater reduction in power per mode when SSD bandwidth is introduced. The rms modulation is reduced by a factor of about four, between the static and 0.33-THz cases from a measured rms of 0.6 to 0.15. For a mode number of 67, the optical power per mode is reduced a factor of 30 to 35, and it is reduced a factor of 20 to 25 at mode 20 with 0.33-THz SSD.

We used the 2-D LASNEX computer code to simulate the imprint of a thin Si foil in a 2-D approximation. We simulated imprint on a target 60 μm wide in the transverse direction with reflection boundary conditions. The laser intensity and pulse shape were taken from the experiments, but the drive pattern was calculated from a speckle model[18] at each time step. For the example of zero bandwidth, the lineout was static, whereas for the case with the SSD-smoothed imprint beam, the speckle pattern was calculated at each time step in the simulation, and this time-varying lineout across the dispersion direction was used as the laser intensity profile for the simulation.

The rms modulation in optical depth was calculated and averaged over 80 ps, centered at t = 260 ps. As shown in Fig. 5, the result was convolved with a 1-D MTF for the imaging system for comparison with the experiment. The rms modulation of the optical depth of the Si foil calculated for the static speckle pattern imprint is 0.36. For the 0.33-THz SSD smoothed speckle pattern, the imprinted rms modulation from the simulation is 0.072, about a factor of five lower than the static case. This is consistent with the reduction in rms modulation of the asymptotic optical intensity distribution, shown in Fig. 5 for comparison. (We have not included the effect of the 100-ps skew in the imprinting laser beam in the simulation. Results from applying the skew parallel or perpendicular to the dispersion direction indicate that it reduces the rms modulation by a factor less than two for each case.)

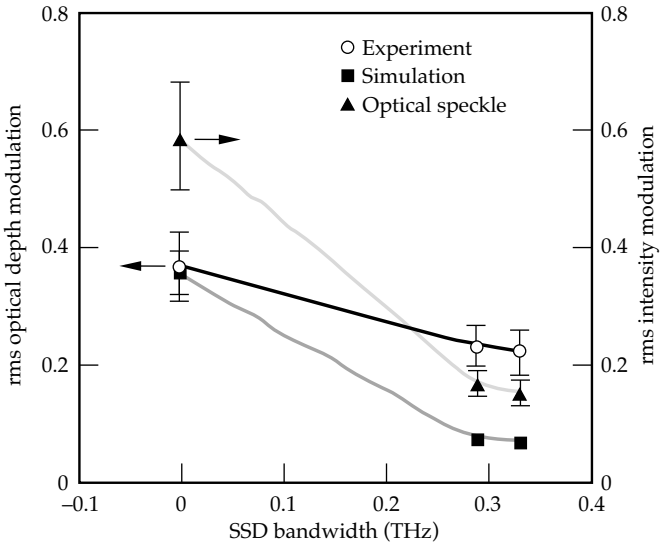

FIGURE 5. Simulated rms modulation in optical depth imprinted in the Si foil. Optical rms and experimental results are included. (08-00-0296-0367pb01)

Figure 5 also plots the measured rms modulation of the Si foil. The simulated imprint decreases more rapidly with SSD bandwidth than we measured using XUV radiography. To test whether the conclusion is affected by noise in the measurement at high mode number, we impose a high-mode cutoff in calculating the rms modulation. The result does not change significantly. By integrating only over modes with mode numbers less than 24 (λ < 5 μm), the measured rms modulation of the imprint is reduced by a factor of 1.7 when we apply SSD bandwidth. The simulated rms is reduced by a factor of 4.5 by the addition of SSD smoothing.

The difference between reduction of optical and imprinted hydrodynamic perturbations through SSD smoothing is important in assessing the effectiveness of SSD bandwidth for suppression of imprint. We expect that the hydrodynamic response of the Si target should be linear with the optical intensity modulation, but the temporal weighting of the optical speckle may be more complex than is indicated by just the time-averaged speckle pattern. This may be due to the presence of the skew in the beam and the finite rise time of the laser pulse shape. The fact that the measured imprint is reduced less than the asymptotic laser smoothing level suggests that the observed imprint is dominated by the early time intensity modulation in the optical speckle pattern, before the asymptotic limit is reached. This limit is reached for the SSD-smoothed beam by about 100 ps,[18] which implies that the imprinting time for the short spatial scales measured here is significantly shorter than 100 ps. One possible reason is that the effect of thermal smoothing may be progressively overwhelming the effect of the optical smoothing, though the 2-D modeling implicitly includes thermal smoothing.

The simulations also show less reduction in the imprint than the optical smoothing level. A similar experimental conclusion has been obtained in parallel measurements using conventional x-ray radiography.[19]

Summary

We measured laser imprint as the modulation in optical depth of a thin Si foil that is irradiated by a low-intensity 0.35-μm beam on Nova. We recorded images of imprint due to a beam with and without SSD bandwidth by using an x-ray laser backlighter, and we demonstrated the effect of beam smoothing on laser imprint at the time of shock breakout.

The imprinted rms modulation in optical depth is reduced by a factor of two when the time-integrated rms modulation in exposure of the optical drive pulse is reduced by a factor of seven from 1.0 to 0.15 with 0.33-THz bandwidth. Simulations of the imprint in two dimensions show about a factor of four reduction in the rms optical depth modulation, also less than the reduction of the optical modulation rms.

Acknowledgments

We gratefully acknowledge the support from the Nova Operations group for their assistance and patience during these experiments. S. Alvarez and J. R. Mazuch assembled the XUV laser targets. J. C. Moreno provided assistance in measuring the absolute x-ray laser timing.

Notes and References

1. J. M. Soures, *J. Fusion Energy* **10**, 295 (1991).
2. J. D. Sethian et al., *Fusion Technology* **26**, 717 (1994).
3. S. W. Haan et al., *Phys. Plasmas* **2**, 2480 (1995).
4. J. D. Kilkenny et al., *Phys. Plasmas* **1**, 1379 (1994).
5. M. H. Desselberger et al., *Phys. Rev. Lett*. **68**, 1539 (1992).
6. M. H. Emery et al., *Phys. Fluids B* **3**, 2640 (1991).
7. S. Skupsky et al., *J. Appl. Phys*. **66**, 3456 (1989).
8. Y. Kato et al., *Phys. Rev. Lett*. **53**, 1057 (1984).
9. E. M. Campbell et al., *Rev. Sci. Instrum*. **57**, 2101 (1986).
10. L. B. DaSilva et al., *Opt. Lett*. **18**, 1174 (1993).
11. L. B. DaSilva et al., *Rev. Sci. Instrum*. **66**, 574 (1995).
12. T. W. Barbee, Jr., et al., *Appl. Opt.* **32**, 4825 (1993).
13. M. H. Key et al., *J. Quant. Spectrosc. Radiat. Transfer*, **54**, 221 (1995).
14. M. H. Key et al., *XUV Lasers and Applications* 2520 279 (SPIE, Bellingham, WA, 1995).
15. D. H. Kalantar et al., *Rev. Sci. Instrum*. **67**, 781 (1996).
16. G. B. Zimmerman and W. L. Kruer, *Comments Plasma Phys. Controlled Fusion* **2**, 51 (1975).
17. J. W. Goodman, "Statistical Properties of Speckle Patterns," in *Laser Speckle and Related Phenomena*, J. C. Dainty, Ed. (Springer, New York, 1990), Ch. 2, pp. 9–75.
18. S. N. Dixit, Lawrence Livermore National Laboratory, Livermore, CA, private communication (1995).
19. S. G. Glendinning et al., "Measurements of Laser Speckle Induced Perturbations in Laser Driven Foils," Lawrence Livermore National Laboratory, Livermore, CA, UCRL-JC-123082; accepted for publication in *Phys. Rev. E* (1996).